



# A Compact Dual-polarized Probe-fed UWB Antenna System for Breast Cancer Detection Applications

Vanishree R Nawati<sup>1</sup> · B. K. Sujatha<sup>1</sup> · G. S. Karthikeya<sup>2</sup> · Arpan Desai<sup>3,4</sup> · Heng Tung Hsu<sup>5</sup> · Merih Palandoken<sup>6</sup> 

Accepted: 8 March 2024  
© The Author(s) 2024

## Abstract

This article proposes an electrically small, probe-fed Ultra-Wideband (UWB) monopole antenna on a slotted truncated ground plane for breast cancer detection. The physical footprint of the proposed antenna element is 33 mm × 35 mm × 0.5 mm. This element is designed on the low-cost FR4 Epoxy substrate with a thickness of 0.5 mm. The proposed antenna has an electrical size of  $0.33\lambda \times 0.35\lambda \times 0.005\lambda$  at the lowest frequency of operation; the radiator offers an impedance bandwidth of 8.34 GHz, which implies a fractional bandwidth of 115.5%. A compact dual-polarized antenna topology with two orthogonally placed probe-fed monopole antennas is proposed to achieve polarization diversity. The impedance characteristics of the individual radiating elements are maintained in spite of the electrical proximity of the radiators. The numerically computed and experimentally measured results of dual-polarized electrically small UWB antenna agree quite well. The proposed dual-polarized antenna topology is investigated for its utility in breast cancer detection in simulation.

**Index terms** Breast cancer detection · Dual-polarized antenna · Electrically small antenna · Probe-Fed · Thin substrate · Ultra-wideband antenna

## 1 Introduction

Breast cancer, a widespread affliction affecting a substantial population [1], stands as one of the most prevalent global cancer types, with an estimated two million patients [2]. The importance of early detection cannot be overstated, as it plays a pivotal role in monitoring and treating cancerous cells within breast tissue [3]. However, the current screening method, breast mammography, is both cumbersome and expensive, restricting its feasibility for large-scale screening [4]. This article proposes a microwave-based breast cancer detection system, recognizing the need for a cost-effective alternative.

In addressing the antenna design requirements for breast cancer detection, considerations such as smaller dimensions, wide impedance bandwidth, and efficient power coupling to the breast tissue are crucial [5]. While smaller antenna dimensions contribute to compact detection systems, they present a challenge in achieving lower frequencies of operation [6]. It's essential to note that the selection of antennas for specific applications, including breast cancer detection, hinges on factors like frequency of operation, desired resolution, and precise imaging requirements. Monopole antennas [7–11], known for their advantageous attributes,

✉ Merih Palandoken  
merih.palandoken@ikc.edu.tr

G. S. Karthikeya  
karthikeyaglr@gmail.com

Arpan Desai  
arpandesai@nycu.edu.tw

Heng Tung Hsu  
hthsu@nycu.edu.tw

- <sup>1</sup> Department of Electronics and Telecommunication, Ramaiah Institute of Technology, Karnataka 560054, India
- <sup>2</sup> Advanced RF and Wireless Communication Lab, Department of Electronics and Communication, BMS College of Engineering, Karnataka 560019, India
- <sup>3</sup> Industry Academia Innovation School, National Yang Ming Chiao Tung University, Hsinchu, Taiwan
- <sup>4</sup> Department of Electronics and Communication Engineering, CSPIT, Charotar University of Science and Technology (CHARUSAT), Changa 388421, India
- <sup>5</sup> International College of Semiconductor Technology, National Yang Ming Chiao Tung University, Hsinchu, Taiwan
- <sup>6</sup> Department of Electrical and Electronics Engineering, Izmir Katip Celebi University, Izmir 35620, Turkey

are particularly suitable for applications like breast cancer detection. However, the proposed UWB monopole antennas lack demonstrated applications in breast cancer detection.

Efficient coupling of electromagnetic power to breast tissue is vital for tumor detection, favoring probe-feeding techniques over edge feeding or strip line feeding. Consequently, designs using Co-Planar Waveguide (CPW) [7, 8] and strip line edge feeding [9–11] may not be suitable for the application. UWB antennas using probe feeding are proposed in [12–16]. Meanwhile, coaxially fed antennas on low-cost substrates [12] and those designed on Thick felt textile [13] or Taconic substrate [14] entail compromises in bandwidth, dimensions, or cost. The antenna in [15] has a lower 2D profile; however, adding a Dielectric Resonator Antenna (DRA) increases the vertical profile. In contrast, the antenna in [16] employs an all-metal concept, resulting in a significantly larger size. This renders the system impractical for breast cancer detection due to placement issues. Polarization diversity assumes critical importance in enhancing breast cancer detection information. However, existing literature predominantly focuses on bulky single-polarization systems [17].

Recognizing the limitations of microstrip or CPW feeding techniques regarding electrical footprint, this article explores a probe-fed antenna. Furthermore, a novel approach involving orthogonally mounted elements is introduced, paving the way for investigating a compact dual-polarization antenna system. The proposed work delineates key contributions, encompassing the design of an ultra-wideband antenna with an impedance bandwidth of 115.5% on an

electrically thin substrate, a probe antenna with electrically thin characteristics, a dual-polarized antenna system with minimal mutual coupling, and a case study on breast cancer detection using the developed system.

## 2 Probe-fed slotted monopole antenna

The proposed antenna is a probe-fed UWB Monopole antenna designed on an FR4 Epoxy substrate, which is an inexpensive substrate with a thickness of 0.5 mm with a relative dielectric constant ( $\epsilon_r$ ) of 4.4 and a loss tangent ( $\tan \delta$ ) of 0.02. This substrate thickness is equivalent to  $0.005\lambda$  calculated at the lowest frequency of operation, indicating an electrically thin substrate. Typically, the thickness of the substrate and bandwidth have a direct relationship. It is a challenge to achieve higher impedance bandwidth on an electrically thin substrate. The probe-feeding approach enhances the maximum coupling of the incident energy from the antennas to the target tissue. Due to this advantage, the probe-feeding technique was investigated with an electrically thin substrate. The impedance bandwidth of 115% could also be obtained with alternate feeding mechanisms such as edge feed or CPW (Co-planar waveguide) feed. The proposed Probe-fed Monopole antenna has a trident-shaped hexagonal planar radiating patch with hexagonal, rectangular, triangular, and semi-circular slots and modified semi-elliptical ground with semi-circular extension and slots as illustrated in Fig. 1. The overall dimension of the antenna is  $33 \times 35 \times 0.5$  mm, equivalent to  $0.33\lambda \times 0.35\lambda \times 0.005\lambda$

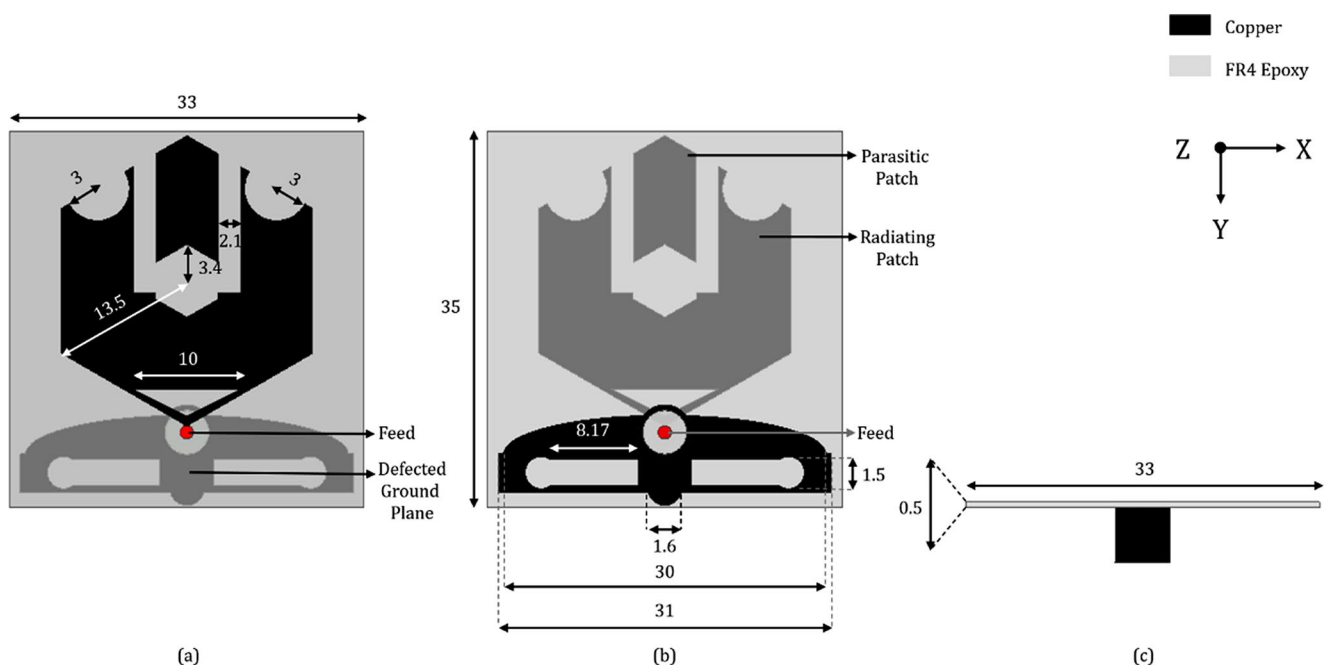


**Fig. 1** Proposed direct-fed UWB monopole antenna (units in mm) (a) top view (b) bottom view (c) side view

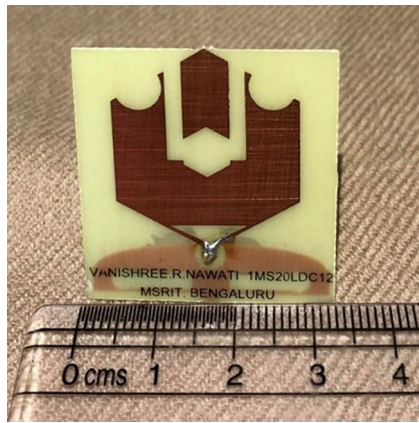


**Fig. 2** Photograph of the fabricated antenna prototype

calculated at the lowest frequency of operation. The photograph of the fabricated antenna prototype is shown in Fig. 2. The proposed antenna is probe-fed using an industry-standard SMA connector. The positioning of the feed determines its input impedance, and the probe's diameter can also impact the performance of the antenna's radiation characteristics. In the proposed antenna, a wideband impedance transformer is designed to match the impedance of the coaxial line to the radiating element. With a conventional hexagonal patch, the fractional bandwidth is nearly 66.67%. Slots must be introduced for bandwidth enhancement on either side of the central frequency. The semi-circular slots with a radius of 3 mm ( $0.03\lambda$ ) are used to enhance the impedance bandwidth further. The triangular slot aids in achieving  $|S_{11}| \leq -10$  dB for higher frequencies greater than 6.35 GHz. The parasitic patch is formed with the intersection of a 3.4 mm ( $0.034\lambda$ ) regular hexagonal slot and rectangular slots of width 2.1 mm ( $0.021\lambda$ ). With an overall size of the parasitic patch

being  $5.8 \text{ mm} \times 11.77 \text{ mm}$ , equivalent to  $0.058\lambda \times 0.1177\lambda$ , it is designed to eliminate the band notches to achieve ultra-wide bandwidth. If a complete ground were considered in the design of the proposed antenna, the antenna would be operational only from 10.78 to 11.22 GHz, offering a bandwidth of merely 0.44 GHz. Thereby, a defective ground structure is taken into consideration. The ground is designed by the intersection of a rectangular structure with a semi-elliptical structure, and it has a semi-circular extension of diameter 1.6 mm ( $0.034\lambda$ ). The overall dimension for the ground is  $31 \text{ mm} \times 8.3 \text{ mm}$  ( $0.31\lambda \times 0.083\lambda$ ) with slots. The slots are used here to achieve impedance matching, with a consequent compromise in the radiation patterns in the operating bandwidth. The E-field patterns for frequencies 3 GHz, 6 GHz, and 9 GHz are shown in Fig. 3.

The parametric results for different slots are presented in Fig. 4. Parametric values 5.4 mm, 3.4 mm, and 2.4 mm were analyzed as measures for the regular hexagon slot. Figure 4(a) shows minimal variations, and 3.4 mm instance is considered the optimal value for the desired impedance bandwidth. Figure 4(b) illustrates the parametric analysis of rectangular slots, and it is observed that with rectangular slots having a width of 2.1 mm, the impedance bandwidth is at its maximum. The parametric analysis of semi-circular slots with radius measures 2 mm, 3 mm, and 4 mm, as shown in Fig. 4(c), has minimal variation but is important for overall bandwidth enhancement. Also, it can be observed that the semi-circular slots with a 3 mm radius offer the largest impedance bandwidth.

The proposed antenna offers a 10 dB impedance bandwidth from 3.07 to 11.41 GHz, offering a bandwidth of 8.34 GHz. The fractional bandwidth is 115.5%. The antenna is fabricated using the industry-standard photo-lithography

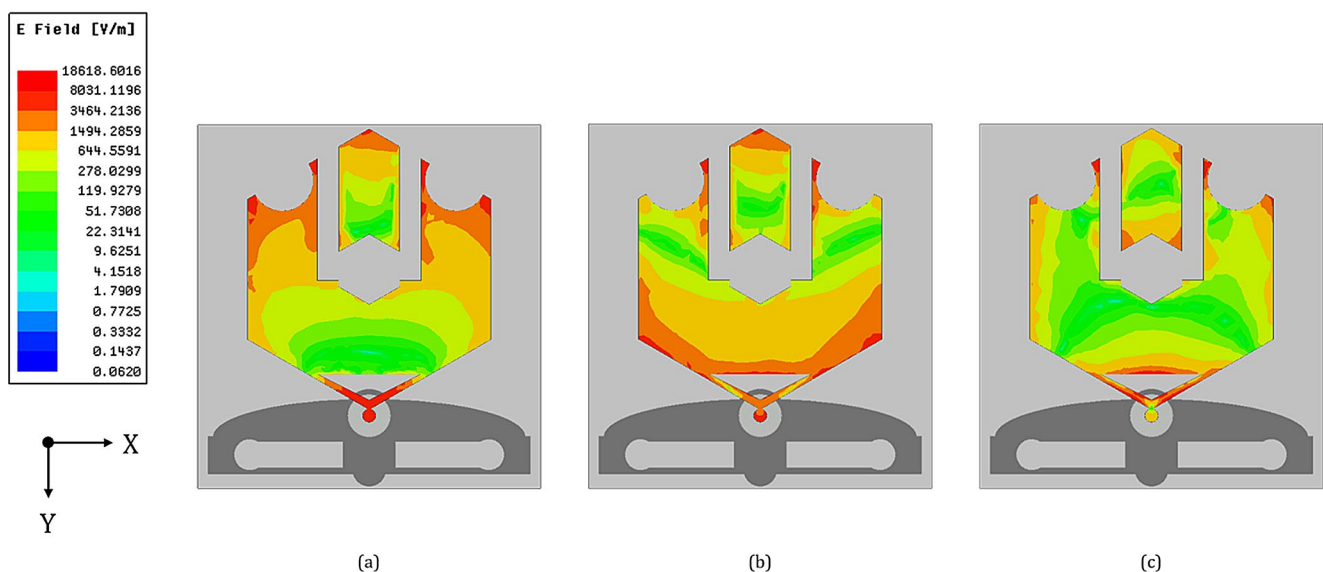


**Fig. 3** E Field patterns for different frequencies (a) 3 GHz, (b) 6 GHz, and (c) 9 GHz

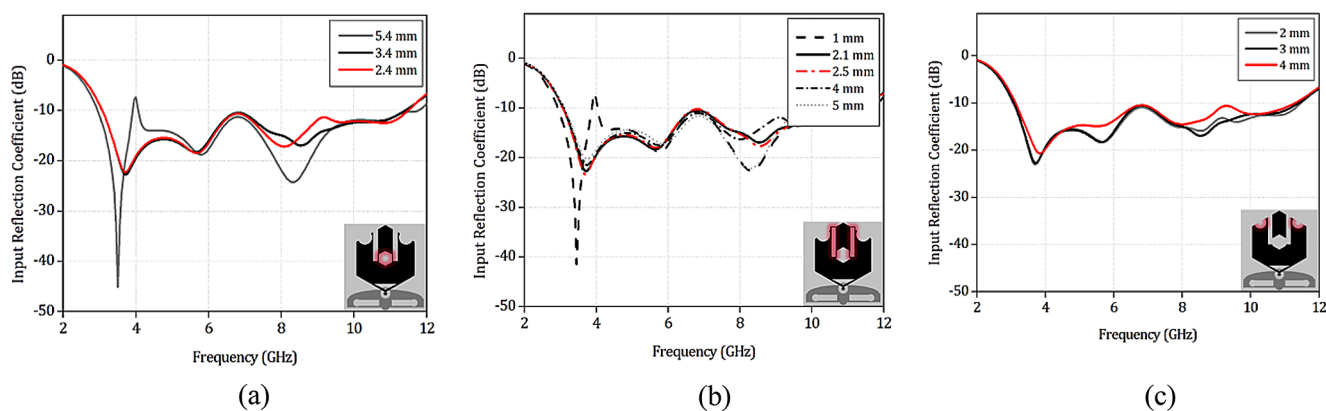


**Fig. 4** Parametric results for  $|S_{11}|$  for different slots of trident-shaped hexagonal planar microstrip antenna (a) hexagonal slot, (b) rectangular slot, and (c) semicircular slot

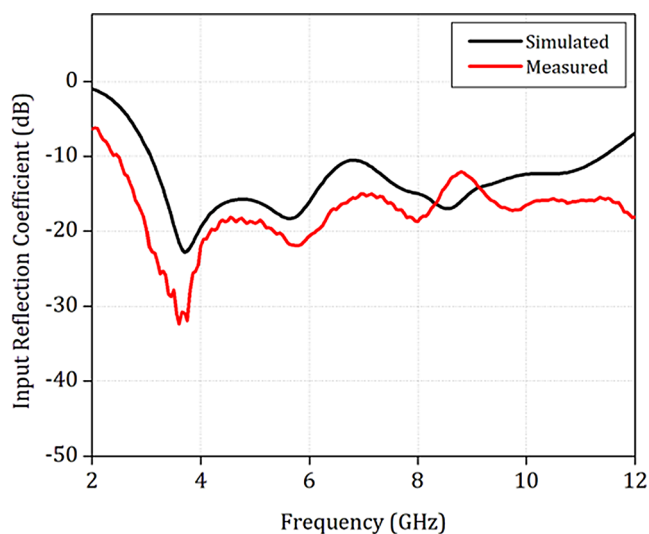


**Fig. 5** Simulated and measured input reflection coefficient of probed monopole antenna

technique. Post fabrication, the realized antenna is tested, and it offers a larger bandwidth greater than 9.5 GHz with  $|S_{11}| \leq -10\text{dB}$  from 2.5 GHz to beyond 12 GHz. Figure 5 shows the proposed individual antenna's simulated and measured Input Reflection Coefficient. The simulated and measured values of  $|S_{11}|$  agree with the limits of fabrication and measurement tolerances.

The Radiation Pattern plots are illustrated in Figs. 6 and 7. The principal plane cuts demonstrate a reasonable beam width for coupling with the breast cancer tissue.

The proposed antenna offers positive gain across lower frequencies from 3 to 6.67 GHz. The gain versus frequency is illustrated in Fig. 8.

### 3 Dual polarised slotted monopole antenna topology

Enhanced information availability is a crucial requirement in breast cancer detection systems. The dielectric constant behavior of the cancerous tissues might vary with the polarization of the incident wave. Henceforth, a dual antenna topology is proposed to obtain additional information. The requirement is to realize the antenna topology, which can offer polarization diversity with an electrically compact design.

The proposed dual antenna topology has two identical antennas placed perpendicular to each other, as shown in the schematic illustrated in Fig. 9. The Antenna-1's width is aligned with the Antenna-2's length. The two antennas are placed at a minimal distance of 0.5 mm, which translates to  $0.005\lambda$  at 3 GHz, as shown in the schematic in Fig. 10. The distance between Port – 1 and Port – 2 is 13.2 mm, equivalent to  $0.132\lambda$  at 3 GHz. A compact scaffolding structure, bearing dimensions  $38.5 \times 39 \times 37$  mm with 1 mm groove cutting, as shown in Fig. 11, is designed and 3-D printed with PLA material to support the proposed topology for testing. This ensures that the small gap of 0.5 mm between the two antennas is strictly maintained without any impact on the performance of the topology.

The measured values agree with the simulated values within the limits of measurement errors. The polarization diversity is maintained across all frequencies in the impedance bandwidth of 8.48 GHz; the dual antenna topology can be used for breast cancer detection with relatively higher sensitivity.

The proposed dual antenna topology offers an impedance bandwidth of 8.48 GHz with input reflection coefficient,  $|S_{11}| \leq -10$  dB for frequencies ranging from 2.83 to 11.31 GHz and a fractional bandwidth of 119.9%. Figure 12 illustrates the S parameter results for the proposed topology.

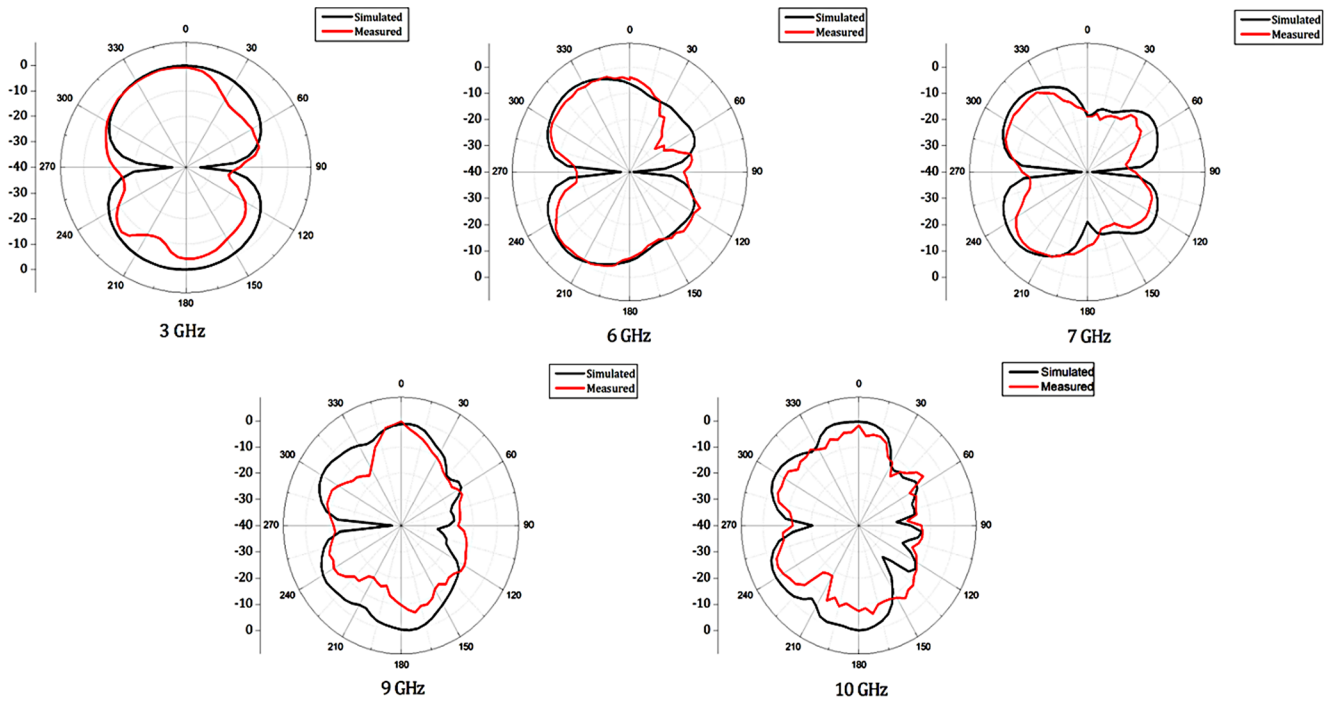


Fig. 6 Simulated and measured XY-plane radiation patterns for various frequencies

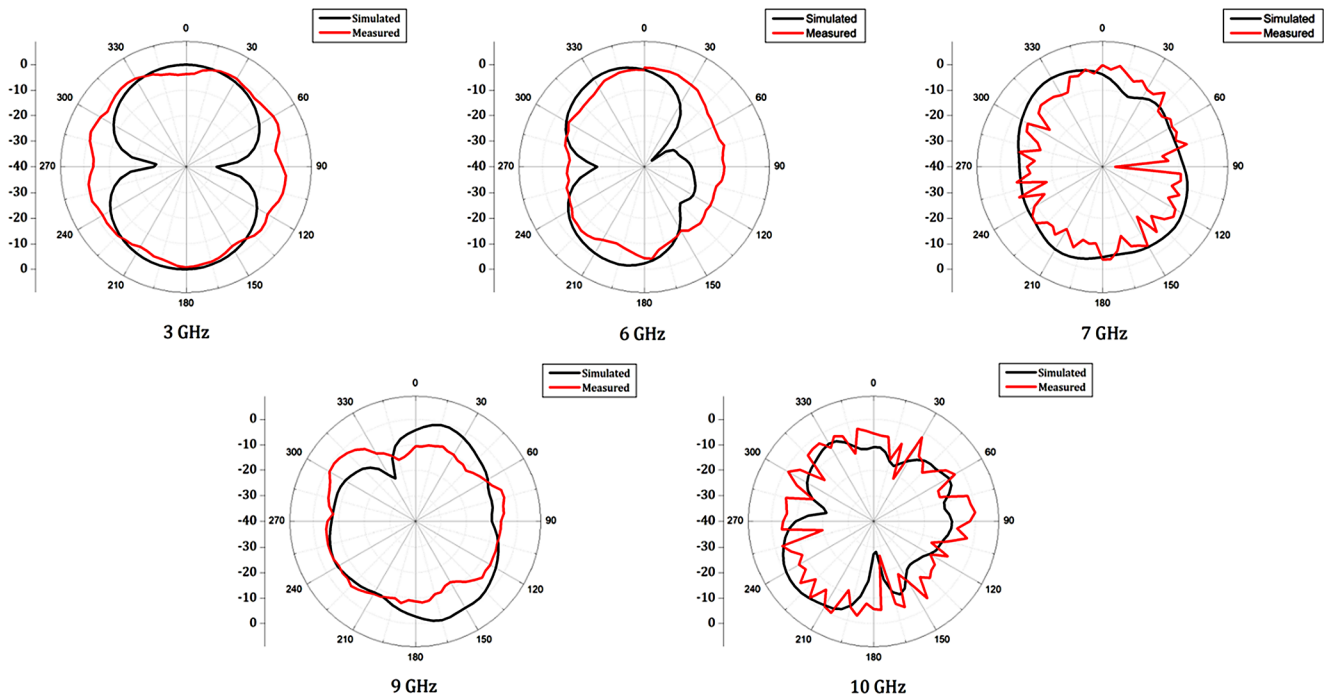


Fig. 7 Simulated and measured YZ – plane radiation pattern for various frequencies

Gain patterns are generated with individual port excitations to confirm the polarization diversity, and the achieved results of the same are presented in Figs. 13, 14, 15, 16 and 17, where subplot (a) is when the port of Antenna – 1 is excited and (b) is when the port of Antenna – 2 is excited.

Gain plots for 3 GHz, 6 GHz, 7 GHz, 9 GHz, and 10 GHz are shown in Figs. 13, 14, 15 and 16, and Fig. 17, respectively.

The patterns differ for different port excitations, illustrating the achieved polarization diversity with the proposed topology using two antennas.



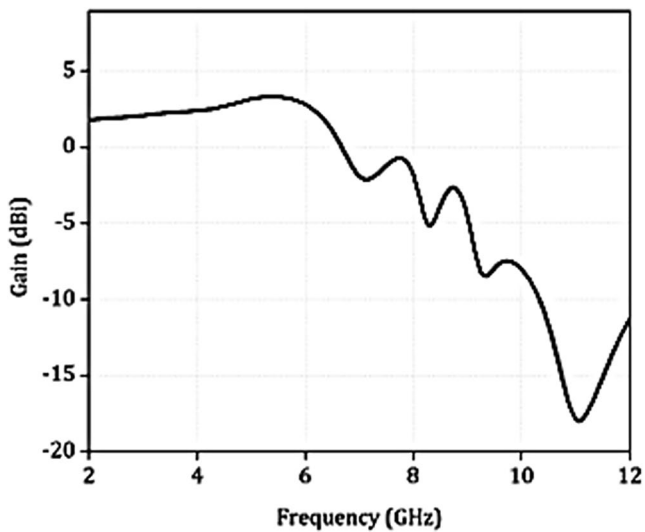


Fig. 8 Gain versus frequency of the proposed antenna element

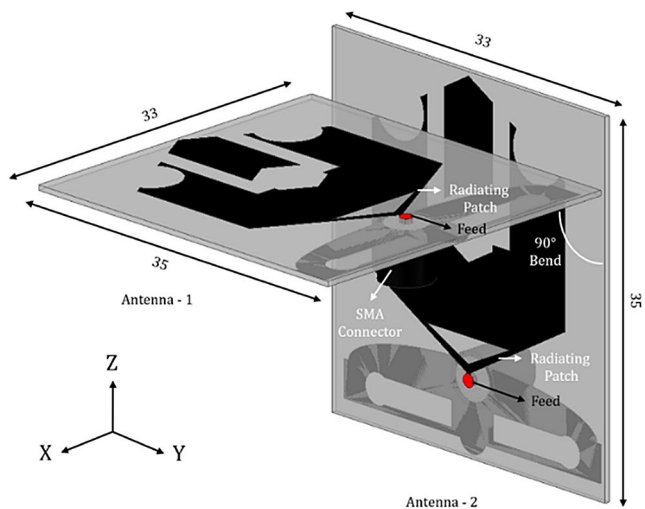


Fig. 9 Proposed dual antenna topology (units in mm)

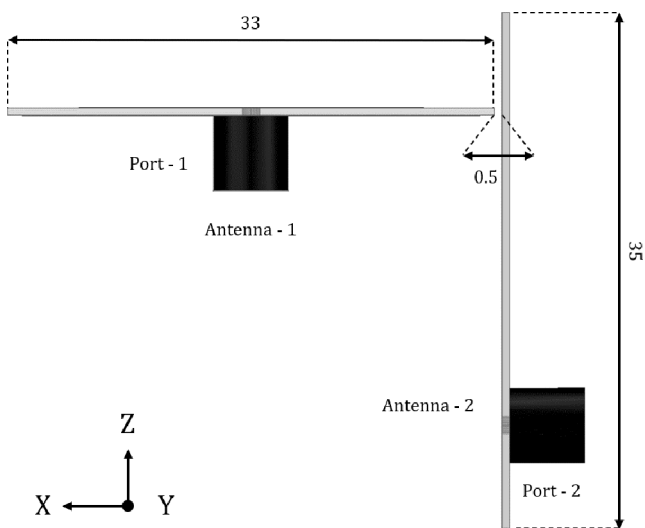


Fig. 10 Side view of the proposed dual antenna topology (units in mm)

### 4 Breast phantom modelling

Breast as a subject for testing is modeled using Ansys® HFSS Electromagnetics Suite, Release 19.2.0. Every human being’s breast size is different, and considering the same, based on the average breast size, the simulation phantom is designed. From [17], the average breast size of an adult woman is 11.4 cm in diameter. The breast is a heterogeneous mass and comprises different layers. The thickness of various layers is taken into consideration for modeling in reference to [18], which suggests that the thickness of the skin is around 1.6 mm, and there is a 10 mm thick layer of fat beyond which is the glandular tissues and muscles. As per multiple statistical analyses, the most common type of breast cancer is found in the glandular tissues. Figure 18(a) illustrates the top view of the modeled breast phantom with three different layers, skin, fat and glandular tissues, and Fig. 18(b) shows the Side View.

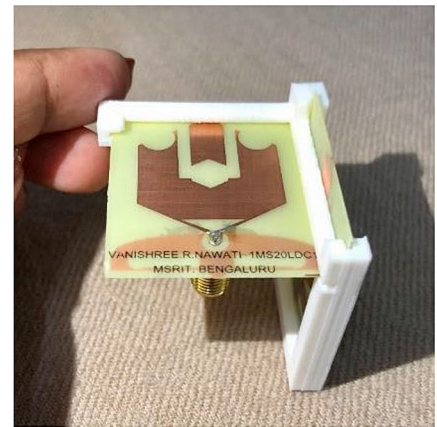
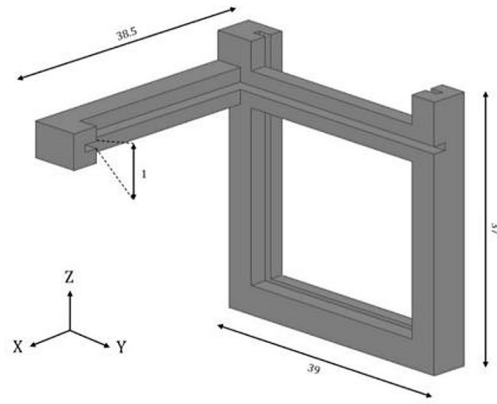
Different layers of the breast have different dielectric properties, which is a function of frequency. We consider 3.7 GHz as the frequency of operation, considering the characteristic performance of the antenna. The dielectric parameters for the layers of the breast are generated using [19], which is based on the Gabriel Dispersion Relationships. Tumor growth has higher cell density, and both types of tumor growth, benign and malignant, have nearly the same dielectric properties. The generated dielectric parameters correspond with the [20] and can be summarized as shown in Table – 1. The isometric view of the modeled breast phantom is illustrated in Fig. 19 with tumor growth (black in color).

### 5 Demonstration for breast cancer detection

Two cases have been devised to study the performance of the proposed antenna and dual antenna topology in breast cancer detection, one with regular breast phantom and the other having tumor. The S parameter values show distinct differences to confirm the presence of a tumor. Figure 20 shows the two cases using a single antenna element and a probe-fed monopole antenna, and Fig. 21 illustrates the two possible scenarios using dual antenna topology.

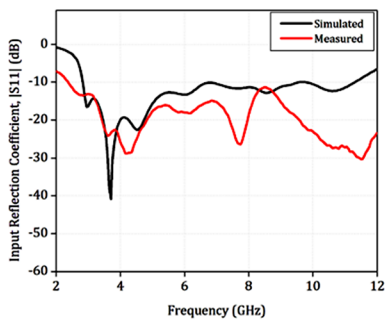
For the antenna single element, the results of |S21| is presented to show the distinguishing difference as illustrated in Fig. 22, and similarly, S Parameters |S13|, |S14|, |S23| and |S24| are compared to notice the clear difference to get a clear overview to determine the presence of tumor/ cancer in Fig. 23. Table 1 illustrates the features of the proposed work compared to the reported studies in scientific publications.

**Fig. 11** (a) Compact Scaffolding structure to support dual antenna topology and (b) Photograph of the fabricated prototype for dual antenna topology

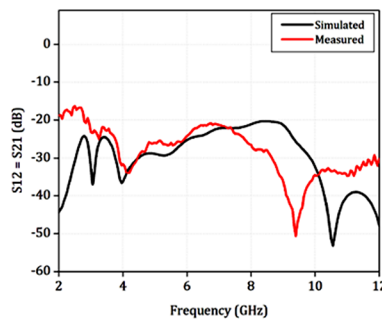


(a)

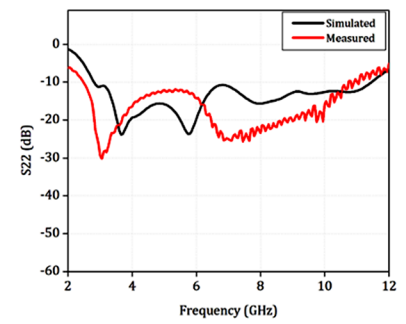
(b)



(a)



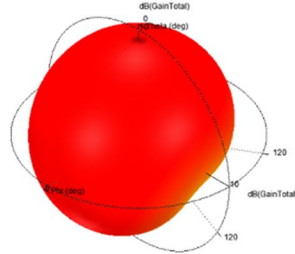
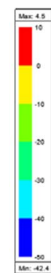
(b)



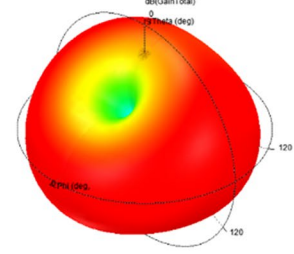
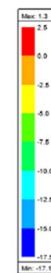
(c)

**Fig. 12** Scattering parameter simulated and measured results for proposed Dual Antenna Topology, (a)  $|S_{11}|$ , (b)  $|S_{12}| = |S_{21}|$  and (c)  $|S_{22}|$  in dB

**Fig. 13** Gain patterns for 3 GHz (a) antenna – 1 Port 1 excited, (b) antenna – 2 Port 2 excited



(a)



(b)

**Fig. 14** Gain patterns for 6 GHz  
**(a)** antenna – 1 Port 1 excited, **(b)**  
 antenna – 2 Port 2 excited

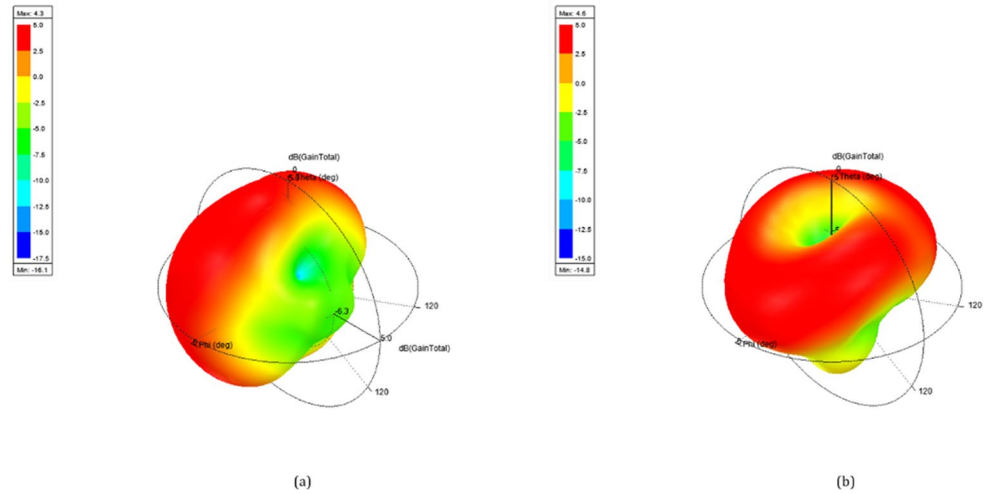


**Fig. 15** Gain patterns for 7 GHz  
**(a)** antenna – 1 port 1 excited, **(b)**  
 antenna – 2 port 2 excited

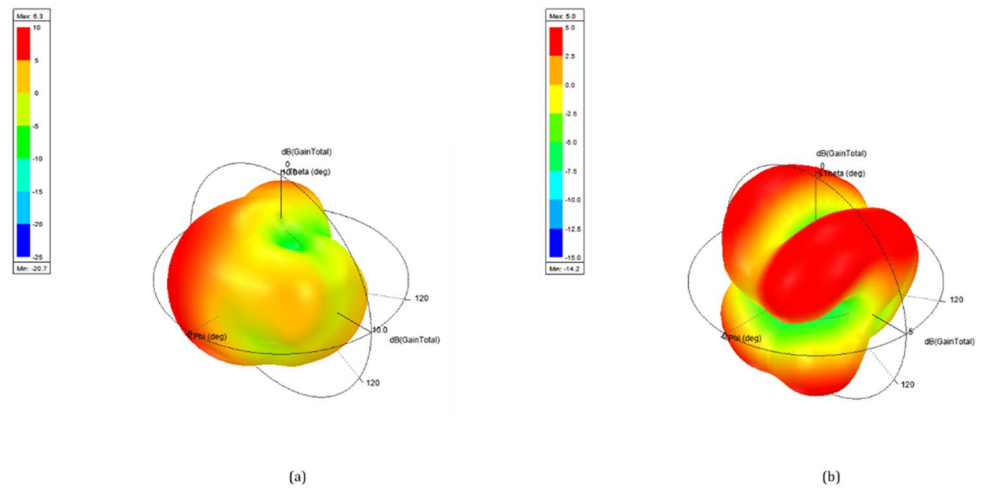


**Fig. 16** Gain patterns for 9 GHz  
**(a)** antenna – 1 port 1 excited, **(b)**  
 antenna – 2 port 2 excited

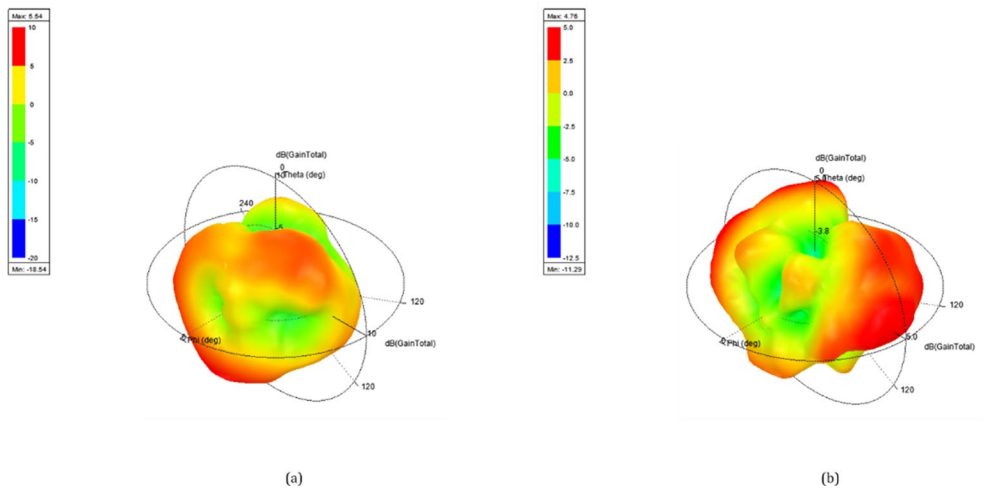
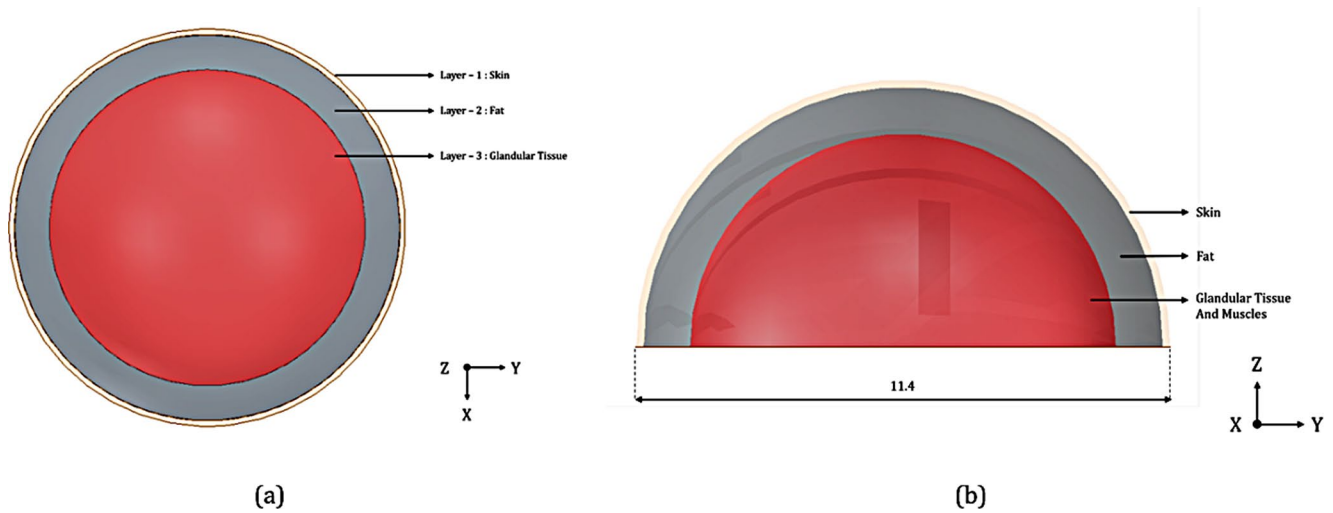
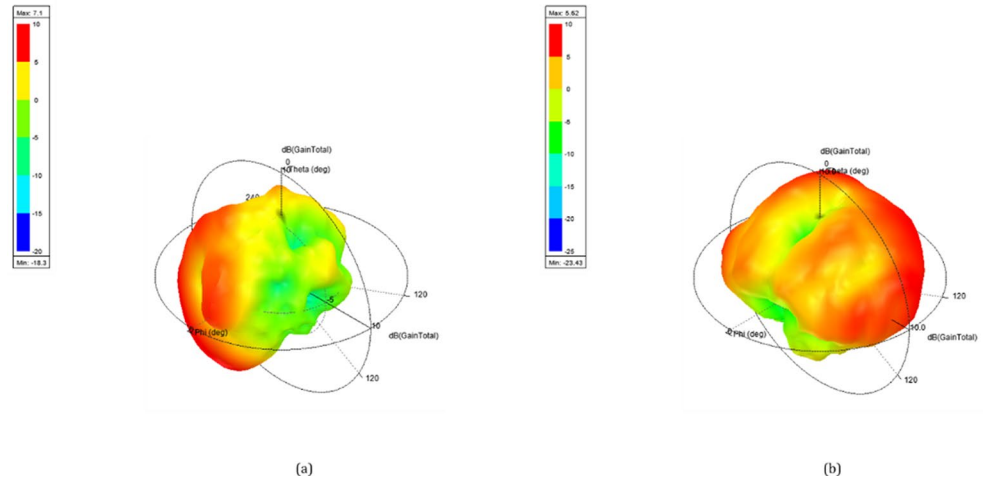


Table 2 presents a comparative analysis of the proposed dual-polarized antenna system with other relevant studies. Our examination reveals that the proposed system exhibits a significantly lower profile than all reported works with dual polarization. This is achieved through the utilization

of a cost-effective substrate. Notably, the antenna system demonstrates commendable characteristics such as a decent Impedance Bandwidth (IBW) and its practical application in breast cancer detection.



**Fig. 17** Gain patterns for 10 GHz (a) antenna – 1 port 1 excited, (b) antenna – 2 port 2 excited



**Fig. 18** Modelled breast phantom showing different layers of the human breast (units in mm), (a) top view and (b) side view

**Table 1** Thickness and dielectric properties of different layers of the breast

Layer of Breast	Thickness in mm	Permittivity	Dielectric Loss Tangent
Skin	1.6	36.8	0.16
Fat	10	4.9	0.93
Glandular Tissue + Muscle	45.4	55.4	0.94
Tumor	≥ 10 (radius)	72.02	1.05

proposed antenna system offers similar impedance characteristics to its constituent antenna elements. It also has minimal mutual coupling between the ports, indicating higher energy coupling from the antenna system to the targeted tissues. An electrically compact dual antenna topology using two identical probe-fed monopole antennas offering dual polarization can be a potential candidate for breast cancer detection or similar applications [21].

## 6 Conclusion

This article proposed an electrically small, probe-fed Ultra-wideband (UWB) monopole antenna with an electrically small, slotted ground structure for breast cancer detection. The proposed antenna element is electrically compact with ultra-high impedance bandwidth. The antenna is realized with the commercial industry standard, low-cost substrate. A dual-polarized antenna system is also investigated. The

**Fig. 19** Isometric view of the modeled breast phantom showing different layers of the human breast with tumor

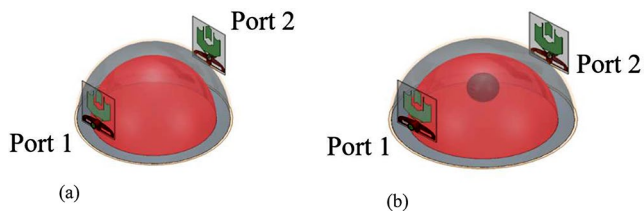
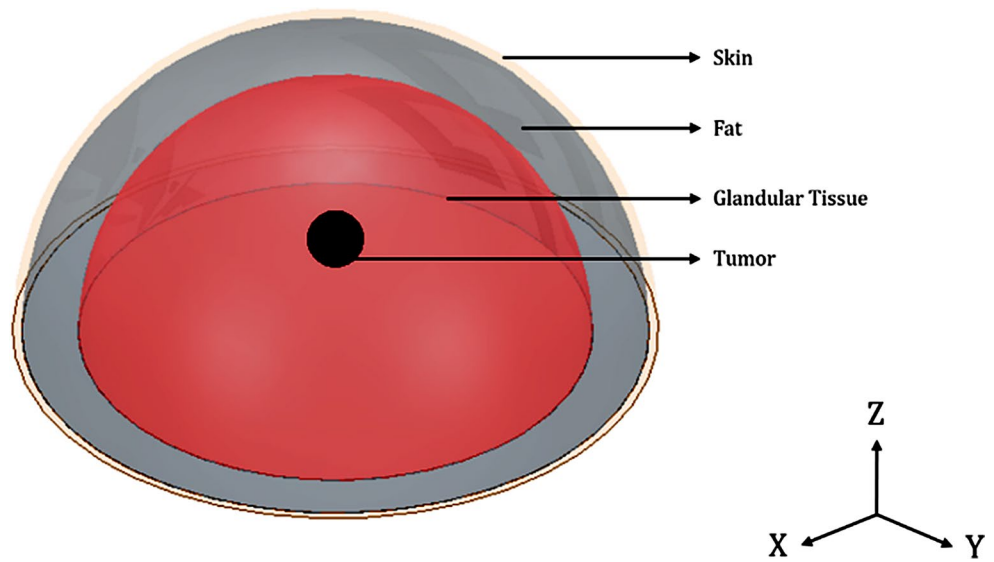


**Fig. 20** Case Study setup for a single element, a probe-fed monopole antenna, (a) case – 1 with regular breast phantom, (b) case – 2 with breast phantom having a tumor

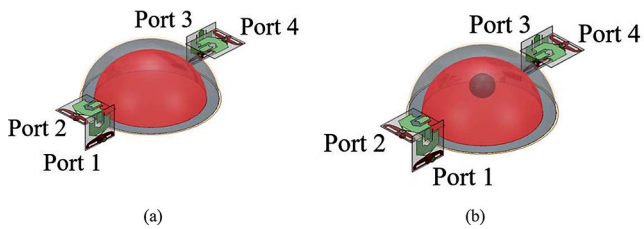


**Fig. 21** Case study setup for dual antenna topology: (a) case – 1 with regular breast phantom, (b) case – 2 with breast phantom having tumor

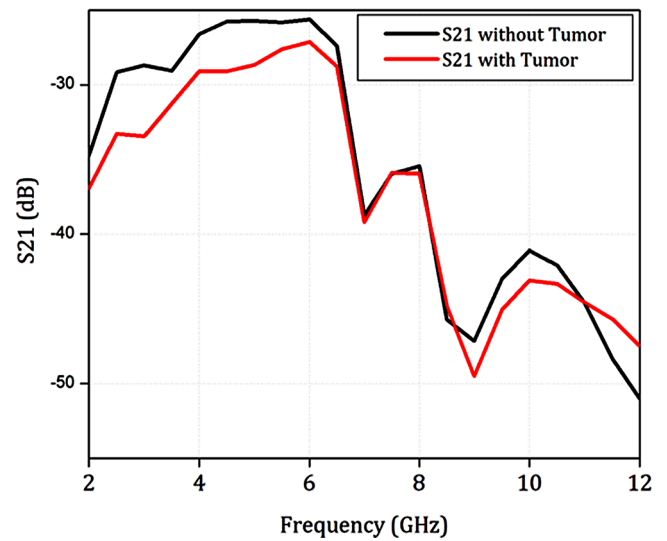


**Fig. 22** Results of  $|S_{21}|$  for different cases in single antenna setup for breast cancer detection

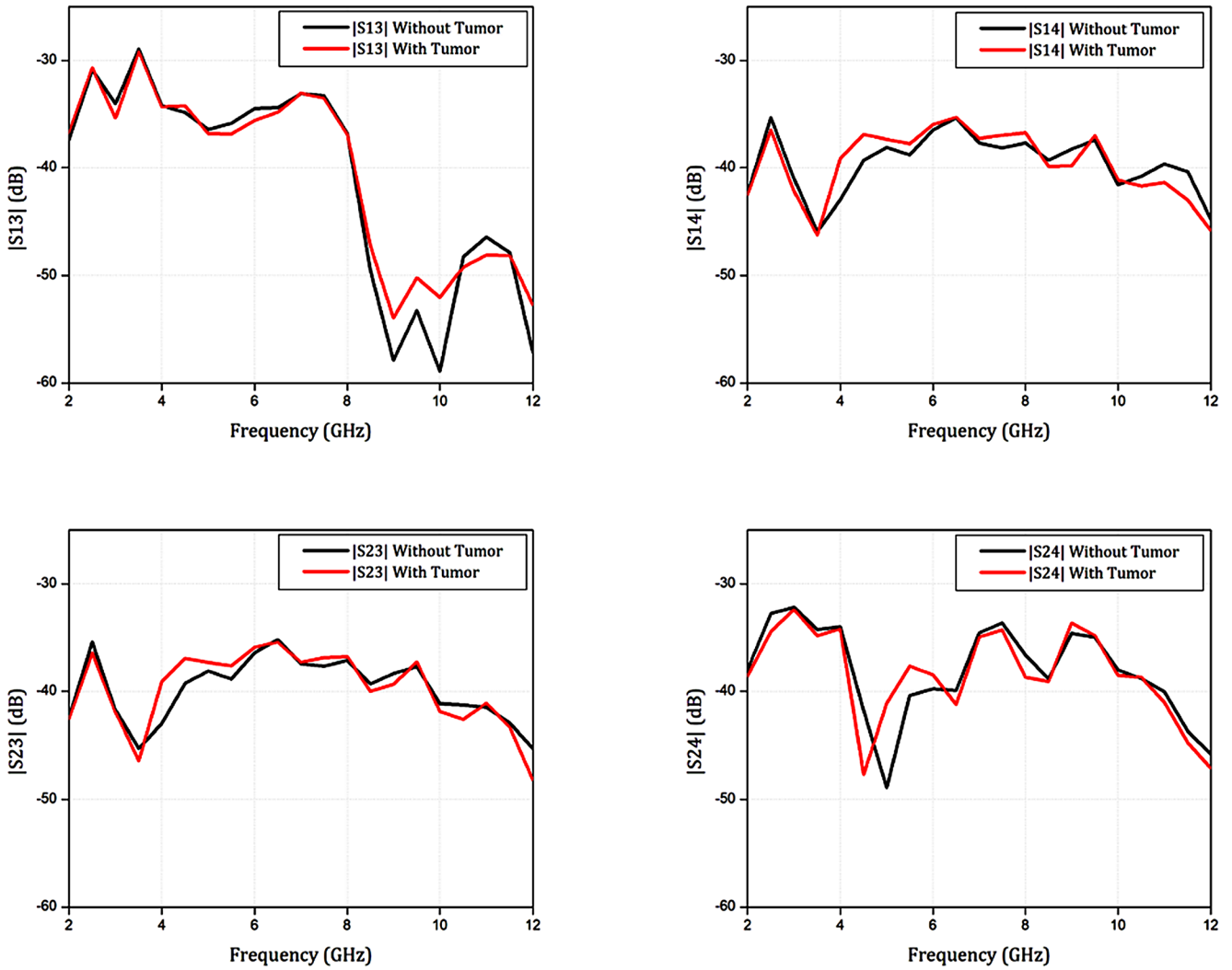


Fig. 23 Results of  $|S_{13}|$ ,  $|S_{14}|$ ,  $|S_{23}|$  an  $|S_{24}|$  for different cases in dual antenna topology setup for breast cancer detection

Table 2 Comparison table with other UWB antenna designs

Ref.	Antenna Dimension (in mm) / (in $\lambda$ )	Substrate	Feed Type	BW in GHz	Fractal BW in %	Application
[12]	46×46×1.57/ 0.353×0.353×0.012	FR4 Epoxy	Coaxial feed	8.3	128 (with band notch)	UWB
[13]	42×39×3/ 0.91×0.845×0.065	Thick felt textile	Coaxial feed	3.4	41.46	UWB
[14]	80×45×1.6/ 0.67×0.38×0.013	Taconic	Coaxial feed	10.1	133.7	Microwave Imaging
[15]	30×40×11.3/ 0.38×0.51×0.145	Rogers TMM10	Coaxial feed	9.45	110	UWB
[16]	150×150×43.5/ 0.7×0.7×0.203	Brass Sheet (All Metal)	Coaxial feed	10	156.25	UWB
Proposed (Single antenna)	33×35×0.5/ 0.33×0.35×0.005	FR4 Epoxy	Coaxial feed	8.34	115.5	Brest Cancer Detection
Dual Antenna Topology	(33×35×0.5) × 2	FR4 Epoxy	Coaxial feed	8.48	119.9	

**Acknowledgements** This research was funded by the National Science and Technology Council, Taiwan, under Grants NSTC 113-2927-I-A49-506-, NSTC 112-2221-E-A49-170-MY2, NSTC 112-2218-E-A49-018, NSTC 112-2622-8-A49-013-SB, NSTC 112-2622-8-002-020, NSTC 113-2634-F-A49-008. The National Science and Technology Council, Taiwan, T-Star Center project “Future Semiconductor Technology Research Center” also financially supported this work.

**Funding** Open access funding provided by the Scientific and Technological Research Council of Türkiye (TÜBİTAK).

**Data availability** The datasets generated during and/or analyzed during the current study are available from the corresponding author upon reasonable request.

**Open Access** This article is licensed under a Creative Commons Attribution 4.0 International License, which permits use, sharing, adaptation, distribution and reproduction in any medium or format, as long as you give appropriate credit to the original author(s) and the source, provide a link to the Creative Commons licence, and indicate if changes were made. The images or other third party material in this article are included in the article’s Creative Commons licence, unless indicated otherwise in a credit line to the material. If material is not included in the article’s Creative Commons licence and your intended use is not permitted by statutory regulation or exceeds the permitted use, you will need to obtain permission directly from the copyright holder. To view a copy of this licence, visit <http://creativecommons.org/licenses/by/4.0/>.

## References

- Qian, L., Bai, J., Huang, Y., Zeebaree, D.Q., Saffari, A., & Zebari, D.A., (2024). Breast cancer diagnosis using evolving deep convolutional neural network based on hybrid extreme learning machine technique and improved chimp optimization algorithm. *Biomedical Signal Processing and Control* 87, Part A.
- <https://www.who.int/news-room/fact-sheets/detail/breast-cancer#:~:text=Scope%20of%20the%20problem,the%20world's%20most%20prevalent%20cancer>.
- Li, J., Zhou, J., Wang, H., et al. (2023). *Trends in disparities and transitions of treatment in patients with early breast Cancer in China and the US, 2011 to 2021*. JAMA Netw Open.
- Jain, S. (2024). A feasibility study for Biomedical Applications via Microwave Imaging. *Advances in Microwave Engineering* (pp. 287–296). CRC.
- Bahraniabarghouei, H., Porter, E., & Santorelli, A. (2015). Benoit Gosselin, Milica Popović, and Leslie A. Rusch. Flexible 16 antenna array for microwave breast cancer detection. *IEEE Transactions on Biomedical Engineering*, 62(10), 2516–2525.
- Islam, M., Tariqul, M. Z., Mahmud, N., Misran, J. I., Takada, & Mengu Cho. (2017). Microwave breast phantom measurement system with compact side slotted directional antenna. *IEEE Access*, 5, 5321–5330.
- Desai, A., Kulkarni, J., Kamruzzaman, M. M., Hubálovský, Š., Hsu, H. T., & Ibrahim, A. A. (2022). Interconnected CPW Fed Flexible 4-Port MIMO Antenna for UWB, X, and Ku Band Applications, in *IEEE Access*, vol. 10, pp. 57641–57654, <https://doi.org/10.1109/ACCESS.2022.3179005>.
- Patel, A., Desai, A., Elfergani, I., Vala, A., Mewada, H., Mahant, K., Patel, S., & Zebiri, C. (2022). Jonathan Rodriguez, and Esraa Ali. UWB CPW fed 4-port connected ground MIMO antenna for sub-millimeter-wave 5G applications. *Alexandria Engineering Journal*, 61(9), 6645–6658.
- Alsath, M. G. N., & Kanagasabai, M. (2015). Compact UWB Monopole Antenna for Automotive Communications, in *IEEE Transactions on Antennas and Propagation*, vol. 63, no. 9, pp. 4204–4208, Sept. <https://doi.org/10.1109/TAP.2015.2447006>.
- Desai, A., Hsu, H. T., Yousef, B. M., Ameen, A. M., Tsao, Y. F., & Ahmed, A. Ibrahim. (2023). UWB connected ground transparent 4-port flexible MIMO antenna for IoT applications. *IEEE Internet of Things Journal*.
- Park, S., & Jung, K. Y. (2022). Novel compact UWB planar monopole antenna using a ribbon-shaped slot, in *IEEE Access*, vol. 10, pp. 61951–61959, <https://doi.org/10.1109/ACCESS.2022.3182443>.
- Joshi, A. (2020). Probe-fed hexagonal ultra wideband antenna using flangeless SMA connector. *Wireless Personal Communications*, 110(2), 973–982.
- Samal, P. B. (2019). Ping Jack Soh, and Zahriladha Zakaria. Compact and wearable microstrip-based textile antenna with full ground plane designed for WBAN-UWB 802.15. 6 application. In *13th European Conference on Antennas and Propagation (EuCAP)*, pp. 1–4. IEEE, 2019.
- Jamlos, M. A. (2015). Mohd Faizal Jamlos, and Abdul Hafizh Ismail. High performance of coaxial feed UWB antenna with parasitic element for microwave imaging. *Microwave and Optical Technology Letters*, 57(3), 649–653.
- Abushakra, F., Al-Zoubi, A., Uluer, I., & Derar Hawatmeh. (2021). Ultra-wideband E-shaped dielectric resonator antenna fed by coaxial probe and trapezoidal conductor. *International Journal of Electronics Letters*, 9(2), 246–255.
- Wong, K. L., Wu, C. H., & Su, S. W. (2005). Ultrawide-band square planar metal-plate monopole antenna with a trident-shaped feeding strip. *IEEE Transactions on Antennas and Propagation*, 53(4), 1262–1269.
- Bra size, & Wikipedia The Free Encyclopedia, 25-Apr-2022. [Online]. Available: [https://en.wikipedia.org/w/index.php?title=Bra\\_size&oldid=1084596998](https://en.wikipedia.org/w/index.php?title=Bra_size&oldid=1084596998). [Accessed: 25-Apr-2022].
- Katbay, Z., Mokdad, S. A., Sadek, S., Le Roy, M., Lababidi, R., & Pérennec, A. (2017). A UWB Antenna in direct breast contact for cancer detection. *2017 Sensors Networks Smart and Emerging technologies (SENSET)* (pp. 1–4). IEEE.
- Dielectric Properties Itis.swiss. [Online]. Available: <https://itis.swiss/virtual-population/tissue-properties/database/dielectric-properties/>. [Accessed: 01-Nov-2021].
- Khuda, I. E. (2017). A comprehensive review on design and development of human breast phantoms for ultra-wide band breast cancer imaging systems. *Engineering Journal*, 21(3), 183–206.
- Kim, I., Lee, D. M., Lee, Y. J., Shin, J. W., Kim, E. S., & Lee, H. (2022). Dual-band on-body near field antenna for measuring deep core temperature with a microwave radiometer. *Ieee Access : Practical Innovations, Open Solutions*, 10, 63715–63722.

**Publisher’s Note** Springer Nature remains neutral with regard to jurisdictional claims in published maps and institutional affiliations.